Validation of Models for Depletion in High Contrast Systems

Introduction

Upscaling of high-resolution geologic models is a useful technique to improve computational flow simulation efficiency, with the challenges of retaining model heterogeneity and subsurface uncertainty. This work extends the recently developed diffuse source upscaling techniques for high contrast systems, (Liu et al. 2022, Nunna et al. 2019) to pressure transient models of flow, and to determine the impact of averaging sub-volume on the flow capacity (half-cell transmissibility). Examples from selected layers in the SPE 10 benchmark model are presented to demonstrate the concepts.

Methodology: Transient Solutions

The diffusivity equation, Eq. (1), describes pressure transients within a reservoir, or at the scale of an upscaling region, with uniform and constant fluid viscosity and total compressibility.

$$\phi(\vec{x})c_t\frac{\partial p}{\partial t}+\nabla\cdot\vec{u}=0,\quad \vec{u}=-\frac{1}{\mu}\vec{\vec{k}}(\vec{x})\cdot\nabla p \tag{1}$$

The asymptotic solution of the high frequency limit of the Fourier transform leads to the Eikonal equation for the diffusive time of flight (DTOF), $\tau(\vec{x})$ (Virieux et al. 1994).

$$\nabla\tau(\vec{x})\cdot\vec{\vec{k}}(\vec{x})\cdot\nabla\tau(\vec{x})=\phi(\vec{x})\mu c_t \tag{2}$$

The DTOF will characterize the transient solutions of the diffusivity equation.
We utilize finite volume discretizations for each of these equations. The diffusivity equation is formulated using a fully implicit, single time step discretization with a uniform initial reference pressure, $p_{init}=0$. In depletion, one boundary of the upscaling region will be a pressure isobar, $p=p_f$, with no-flow on the remaining boundaries.

$$V_{pi}c_t\frac{p_i-p_{init}}{\Delta t}+\frac{1}{\mu}\sum_{j(i)}T_{ij}\cdot(p_i-p_j)=0 \tag{3}$$

Here, V_{pi} is the pore volume of cell i and T_{ij} is the intercell transmissibility between cell pairs. The Eikonal equation is discretized in terms of the incremental $\delta\tau_{ij}$ for each cell pair.

$$\delta\tau_{ij}=\sqrt{\mu c_t\left(V_{pi}+V_{pj}\right)/\left(2T_{ij}\right)} \tag{4}$$

It is solved using Dijkstra's algorithm (Dijkstra 1959) to obtain the minimum value of the diffusive time of flight at each cell, τ_i, subject to the boundary condition $\tau=0$ on the flowing isobar boundary. Once this solution is obtained, it is characterized in terms of the cumulative pore volume, $V_p(\tau)$.

$$V_p(\tau)=\int_{\tau(\vec{x})<\tau}\phi(\vec{x})d^3x=\sum_{\tau_i<\tau}V_{pi} \tag{5}$$

We now contrast the properties of different solutions to the diffusivity equation. The asymptotic (early time, first passage) pressure solution for a fixed rate drawdown with total flux q_f can be expressed in terms of a diffuse source (Nunna, Liu and King 2019).

$$c_t\frac{\partial p}{\partial t}=-\frac{q_f}{V_d(t)}e^{-\tau^2/4t},\quad V_d(t)=\int_\Omega e^{-\tau^2/4t}dV_p(\tau)=\sum_i V_{pi}\cdot e^{-\tau_i^2/4t} \tag{6}$$

The diffuse source is expressed using the drainage volume, $V_d(t)$, which is a convolution of the cumulative pore volume with the diffusion kernel, $e^{-\tau^2/4t}$, over the domain Ω. A pressure solution for Eq. (3) is obtained over the connected sub-volume for which τ is finite subject to the boundary condition $p_f=0$. Flow capacity is quantified in terms of the face (or half-cell) transmissibility, T_f.

$$1/T_f = \Delta p/\mu q_f, \quad \Delta p = \bar{p} - p_f \tag{7}$$

Here, the pressure $\bar{p}$ is a transmissibility weighted average of the flowing pressure over the upstream faces in the connected sub-volume. In this solution, time is a parameter that needs to be specified, and there is no reference to the initial pressure.

The pressure solution may also be obtained directly from the diffusivity equation, Eq. (3). Now use is made of the initial condition, $p_{init} = 0$ while a pressure isobar of $p_f = -1$ is used to close the equations and determine the flux. Again, the flow capacity is characterized in terms of the face transmissibility, and again the time step size for the discretization remains to be specified.

To specify the time for each of these calculations we utilize additional concepts from the asymptotic pressure solution, Eq. (6), following the earlier references. At a given time, the Limit of Detectability (LOD) is given by $\tau_{LOD}^2/4t = 4$. For $\tau > \tau_{LOD}$ the exponential term in Eq. (6) is negligible and the solution remains close to the initial pressure. In contrast, the Pseudo Steady State (PSS) limit is given by $\tau_{PSS}^2/4t = 0.01$. For $\tau < \tau_{PSS}$ the exponential term in Eq. (6) is close to unity and the solution is locally PSS. The location of the so-called stabilized zone lies within the transient region, $\tau_{PSS} < \tau_{SZ} < \tau_{LOD}$. It is defined by extending the PSS region to match the transient drainage volume $V_p(\tau_{SZ}) = V_d(t)$. For flow simulation purposes we need to characterize the transmissibility at a time for which the well-connected sub-volume of the upscaling region reaches PSS. The extent of this volume is obtained from the median value for τ based on the connected cumulative pore volume (summed over finite τ_i), with the boundary location specified at twice the median value.

$$V_p(\tau_{median}) = \frac{1}{2}\sum_{i}^{Finite\ \tau_i} V_{pi}, \quad \tau_{BND} = 2 \cdot \tau_{median} \tag{8}$$

$$t_{PSS} = 25\tau_{BND}^2 = 100\tau_{median}^2 \tag{9}$$

With this choice of time, the transmissibility is independent of μ and c_t. Pressure averaging of the solution for the transmissibility, Eq. (7), is performed on the furthest upstream extent of the volume defined by τ_{BND}. Dimensionless time $t_D = t/t_{PSS}$ and dimensionless diffusive time of flight $\tau_D = \tau/\tau_{median}$ will be utilized when presenting results.

Example Results

The above methodology has been used to calculate the upscaled face transmissibilities for the 60×220 cells of layer 55 of the SPE10 reference model (Christie and Blunt 2001). 10×10 upscaling is performed providing 132 calculations that may be compared in each of the four face directions, two of which $(\pm J)$ are shown in Figure 1. Steady State (SS) upscaling is used as a reference calculation, in which the isobar pressures are specified on two opposite faces and $\bar{p}$ is defined as the pore volume weighted average of the pressure, here restricted to cells with finite τ. In addition to the PT and DS methods already discussed, the comparisons also include PSS $(t \to \infty)$, LOD (PSS up to τ_{LOD}), SZ (PSS up to τ_{SZ}), and BND (PSS up to τ_{BND}). These results are consistent with previous conclusions:

- Steady state upscaling is biased towards lower transmissibility compared to DS.
- PSS upscaling is even more strongly biased towards lower transmissibility values.

Let us examine one 10×10 upscaling region to get a better sense of the underlying mechanisms. This region has been selected as it provides a good demonstration of the differences between the different calculations.

Permeability and porosity and the directional diffusive time of flight (±J directions) are shown in Figure 2. Cumulative pore volume and the transient drainage volume are in Figure 3. The source term strength

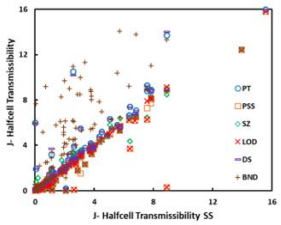

Method	Slope	R^2
PT	1.1636	0.7914
PSS	0.8941	0.9346
SZ	1.0084	0.9786
LOD	0.9042	0.9351
DS	1.1643	0.7911
BND	2.1793	0.6033

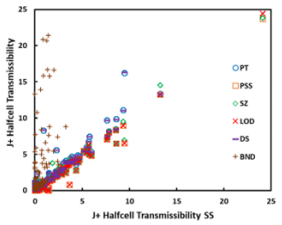

Method	Slope	R^2
PT	1.1485	0.9533
PSS	0.9385	0.9837
SZ	0.9736	0.9844
LOD	0.9482	0.9829
DS	1.1532	0.9525
BND	2.628	0.8309

Figure 1 *Comparison of ±J face transmissibility, SPE 10 layer 55 (10×10 upscaling)*

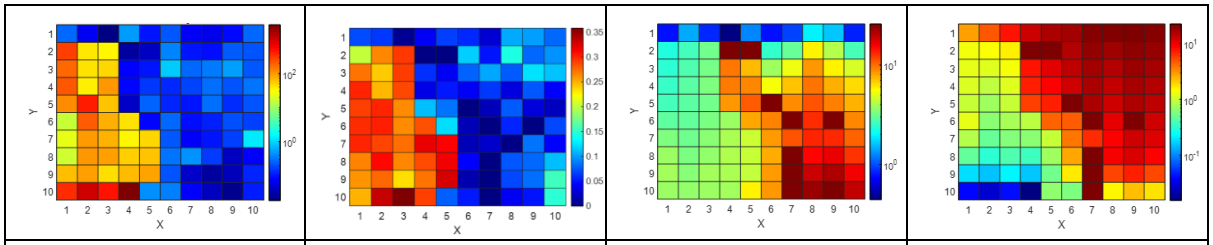

Figure 2 *Permeability, porosity, and ±J directional diffusive time of flight, in the selected region*

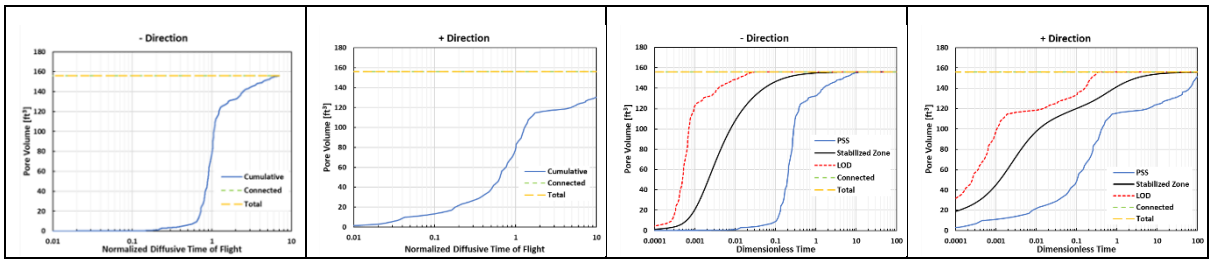

Figure 3 (a)-(d) *Cumulative (left) and transient (right) pore volumes in the J- and J+ directions*

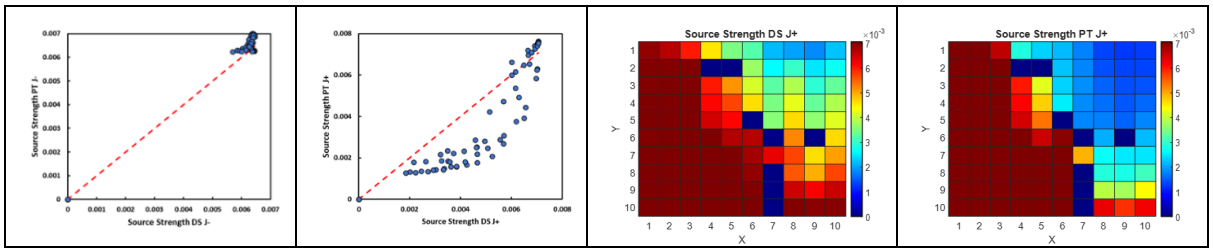

Figure 4 (a)-(d) *Comparison of the PT and DS source terms in the J- direction (left) and J+ direction (right), with additional 2D comparison for the J+ direction*

(normalized to the total flux) of the PT and DS methods are in Figure 4. Figure 2 shows that this upscaling region overlaps a change in facies within the SPE10 geologic description with permeability contrasts of more than four orders of magnitude. The high permeability sub-volume is well connected to the I- and J+ faces but does not extend across the selected upscaling region. The diffusive time of flight provides a characterization of the pressure depletion from each face, here shown for J- and J+. Contours of DTOF show the propagation of the depletion starting from the $\tau = 0$, connecting to the higher permeability cells, and then moving into the lower permeabilities. The cumulative and transient pore volumes in Figure 3 show the impact of the differing spatial patterns, with the J- direction showing good transient connectivity within the upscaling region. In contrast, the depletion geometry of Figure 3(b) and Figure 3(d) show more limited connectivity. Detailed comparison of the pressure solutions is provided in Figure 4. Figure 4(a) compares the source terms (normalized to the total flux) for the PT and DS solutions. Both methods show that almost the entire model reaches PSS, except for a few cells with zero pore volume. In contrast, Figure 4(b)-(d) show consistent deviations. Both methods agree for the zero (isolated) and strong (PSS) source term cells, but they differ for those cells in the transition region. Physically, the asymptotic diffuse source solution is a purely refractive first passage

approximation to pressure depletion that neglects pressure reflections (Rawlinson and Sambridge 2004). Although the transient times associated with the solutions are correct, the long-time amplitudes may be incorrect, as seen in Figure 4(b)-(d), where the DS solution over-estimates the source strength in the less well-connected regions.

Conclusions

Several models of depletion were compared, and flow characterization was obtained for high contrast geologic model (SPE10) upscaling. Diffuse source upscaling was found to be consistent with a new pressure transient upscaling calculation in many of the upscaling regions but may over-estimate the pressure depletion in less well-connected regions. The new PT upscaling approach makes fewer approximations than the DS calculation and is expected to provide improved upscaling accuracy.

Acknowledgments

The authors would like to acknowledge the continuing support of the members of the MCERI joint industry project at Texas A&M University.

References

Christie, M. A. and Blunt, M. J. [2001] Tenth SPE Comparative Solution Project: A Comparison of Upscaling Techniques. SPE Reservoir Evaluation & Engineering 4(04), 308-317.

Dijkstra, E. W. [1959] A note on two problems in connexion with graphs. Numerische Mathematik 1, 269–271.

Liu, C.-H., Nunna, K. and King, M. J. [2022] Application of diffuse source basis functions for improved near well upscaling. Computational Geosciences 26, 823-846.

Nunna, K., Liu, C.-H. and King, M. J. [2019] Application of diffuse source functions for improved flow upscaling. Computational Geosciences.

Rawlinson, N. and Sambridge, M. [2004] Wave front evolution in strongly heterogeneous layered media using the fast marching method. Geophysical Journal International 156(3), 631-647.

Virieux, J., Flores-Luna, C. and Gibert, D. [1994] Asymptotic Theory for Diffusive Electromagnetic Imaging. Geophysical Journal International 119(3), 857-868.